Evaluation of Microstructure Effect on Anisotropic Mechanical Properties of Hot Rolled AZ31 by AE Analysis

Kousuke Matsumoto[1,*], Takashi Yasutomi[1], Manabu Enoki[1]

[1] Department of Materials Engineering, The University of Tokyo, 7-3-1 Hongo, Bunkyo-ku, Tokyo 113-8656, Japan
* Corresponding author: matsumoto@rme.mm.t.u-tokyo.ac.jp

Abstract Anisotropic properties of twinning and slip deformation of hot rolled and extruded AZ31 Mg alloy have been reported in our previous researches. AE (Acoustic Emission) measurement has been done during the tensile test of specimen with various angles between tensile direction and rolled or extruded direction. AE energy had good correlation with twinning area and 0.2% proof stress. It has been also reported that twinning stress has higher grain size dependence than the stress required for activation of slip because the Hall-Petch slope for twinning is larger than that for slip. In this research, tensile test specimen were prepared from rolled AZ31 with various angles between tensile and rolling directions. In order to change grain size of hot rolled AZ31 Mg alloy, the specimens were annealed at various temperatures. Then in-situ measurement of AE signals was conducted during the tensile test. The mechanical deformations occurring actually were found by EBSD (Electron Backscatter diffraction) and observation of fracture surface. According to the result, the effect that grain size of hot rolled AZ31 Mg alloy gives to anisotropic mechanical properties during the tensile test was quantitatively evaluated by AE analysis.

Keywords Acoustic Emission, AZ31, Annealing, Anisotropy, Twinning

1. Introduction

Mg alloy is a light structural metal with high specific strengths; therefore, its alloys are the most attractive materials to be utilized in the automotive and transportation industries. This is due to their lower density compared to that of other structural materials such as steels and aluminum alloys. However, their poor mechanical properties at the room temperature are considered as an important fault. Grain size refinement is a major way to improve mechanical properties. At this point, Hall-Petch relationship predicts that the material strength increases with decreasing grain size. Its hexagonal close-packed structure also characterizes its mechanical properties. In the former research, anisotropic mechanical properties during tensile test of extruded AZ31 Mg alloy is evaluated by AE analysis [1-6]. In this research, the specimens were produced from hot rolled AZ31 Mg alloy with various angles between tensile and rolling directions. These specimen were annealed at various temperatures in order to change their grain sizes. The effect of various grain sizes on mechanical properties was evaluated by AE energy.

2. Experimental procedure

2.1. Material

The material used in this study was hot rolled AZ31 sheet (Mg – 3.04 % Al – 1.06 % Zn – 0.38 % Mn) with a thickness of 3 mm bought from Osaka Fuji Corporation. The as-received specimen had an average grain size of 9.8μm. In order to change grain size, the as-received specimens were annealed at 285°C for 30 min and 450°C for 30 min. The grain sizes after annealing were 13.5 and 17.9μm for the first and latter conditions, respectively.
To study the anisotropy of mechanical properties, the specimens were prepared with various angles between tensile and rolling directions of 0°, 15°, 30°, 45°, 60°, 75° and 90°, shown in Fig. 1. All tests were carried out at a constant strain rate of 1.67×10^{-4} /s.

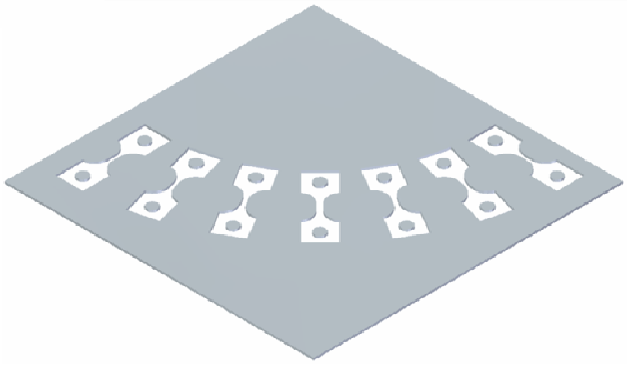

Figure 1. Procedure of cutting specimens

2.2. AE measurement during tensile test

AE measurements were applied with 4 channels in order to remove friction noise from jig of tensile test machine. Positions of AE sensors are shown in Fig. 2. AE sensors used in this study were M304A (Fuji ceramics, Japan). Continuous Waveform Memory (CWM), which was developed by our group, was used to perform AE measurements [7]. The high pass filter was set at 100 kHz. All AE signals are wavelet transformed in order to emphasize dependence of time and frequency. Various threshold levels were set from 60dB to 80dB with an interval of 5dB to detect signals with wide range of amplitude. Then, the data was integrated.

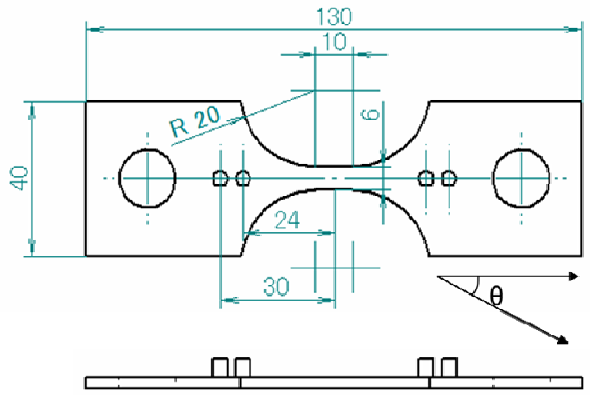

Figure 2. AE sensors positions

2.3. EBSD test

Electron Backscatter Diffraction (EBSD) analysis was performed to evaluate the texture during the tensile testing. The software used in this study was OIM-Analysis 5 of TSL Solutions. Specimens before deformed and after deformed until a strain value of 3% were cut and then polished by a machine called “Cross section Polisher” (CP), which utilizes an argon iron beam to mill the sample. This method prevents any damages from mechanical polishing and therefore the suitable surface for EBSD is easily obtained. Then, automated EBSD scans were performed in the stage control mode with TSL data acquisition software with a step size of 1.5 μm. Average grain size and Schmid factor were calculated from this result. Schmid factor used in this paper is an average value of each grain.

3. Result and discussion

3.1 Microstructure

Initial microstructure of specimens is shown in Fig. 3. As annealing temperature increases, there are less small grains, and the average grain size is larger. Fig 4(a) shows average Schmid factor for twinning of all grains of each angle. In each annealing condition, Schmid factor for twinning is larger at 60° to 90° than another angle. From this tendency, it follows that twinning deformation occurs easily in 60° to 90° specimens. Fig 4(b) shows pole figure for (0002) before tensile test. The (0002) vector shapes ring seen from the RD direction.

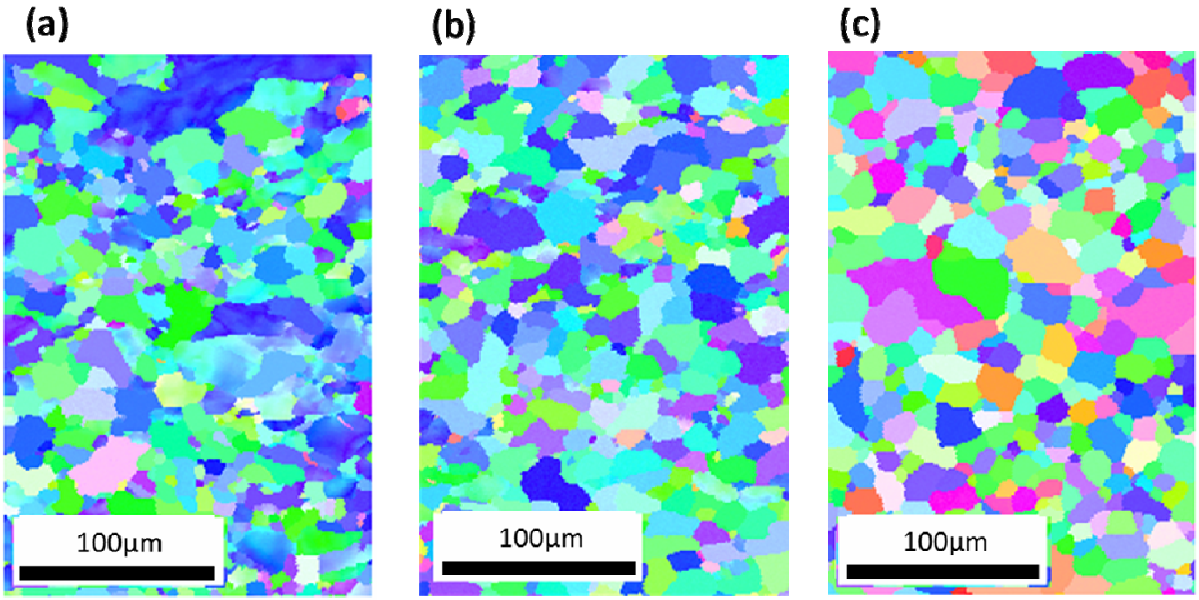

Figure 3. IPF map of (a) as-received, (b) 285°C annealed and (c) 450°C annealed specimens before tensile test

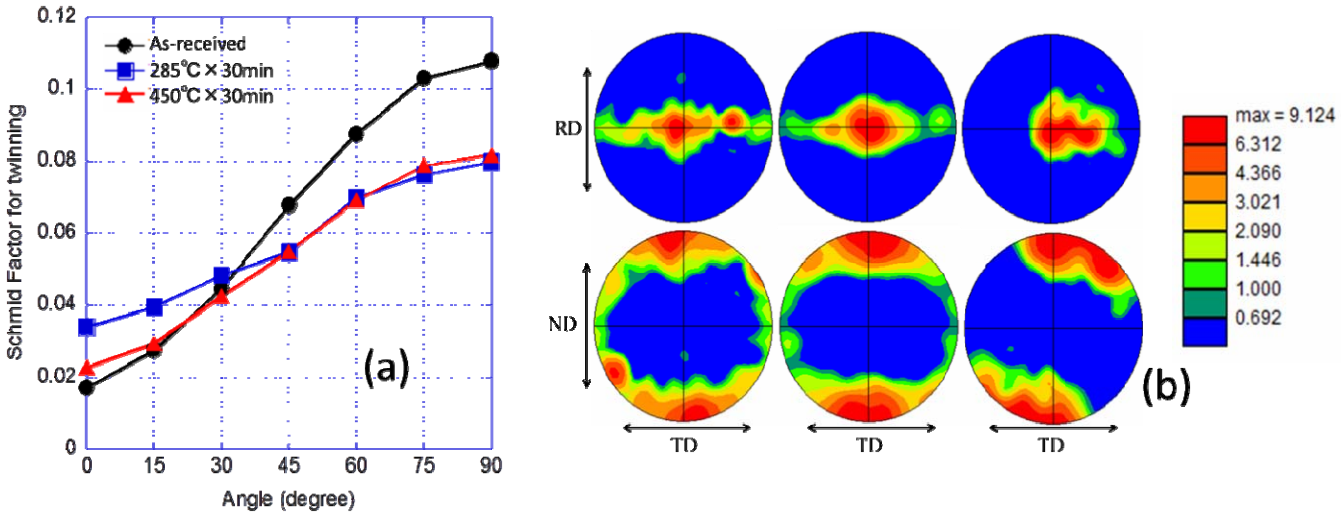

Figure 4. (a) Schmid factor for twinning and (b) pole figure for (0002) before tensile test

3.2. Mechanical properties

Fig. 5 shows strain-stress curve of (a) as-received specimen and (b) 450°C annealed specimen of

each angle. Before and after annealing, nominal stress and strain has different figure in each angle. In other words, strain-stress curve shows anisotropy in each annealing conditions. However, the strength of anisotropy differs by annealing.

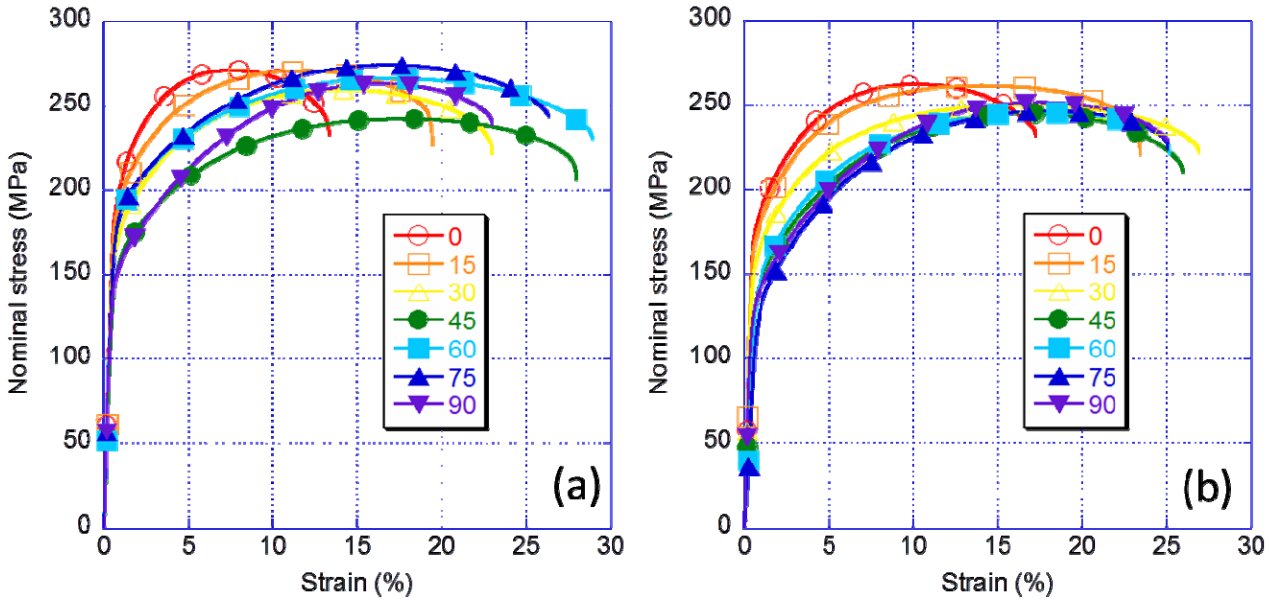

Figure 5. Strain-stress curve of (a) as-received specimen and (b) 450°C annealed specimen

In order to analyze this result, ultimate tensile stress (σ_{max}) and maximum strain (ε_{max}) are plotted in Fig. 6. From Fig. 6(a), ultimate tensile stress is high in 15° and 75°, and is especially low in 45°, so we can see strong anisotropy in as-received specimens. However, in 285° and 450°C annealed specimens, ultimate tensile stress become higher in 45°, and lower in other angles, so it can be said that anisotropy is weakened by annealing. Fig. 6(b) shows that strain also has anisotropy. Strain of as-received specimens is extremely high in 45° to 75°, but by annealing, strain of 0° to 30° becomes higher, on the other hand, strain of 45° to 75° becomes lower. By annealing, strain of 30° to 90° is flat, so it can be said that anisotropy is weaken by annealing.

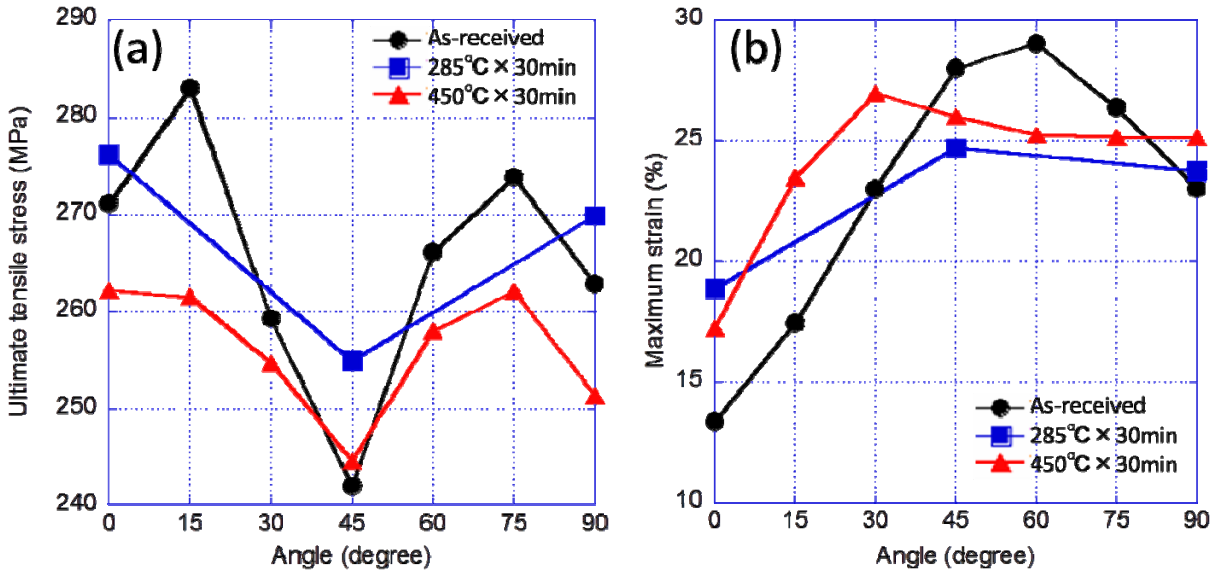

Figure 6. (a) Ultimate tensile stress and (b) Maximum strain of each specimen

However, 0.2% proof stress of each specimens shows different tendency from the former result. Fig. 7 plots 0.2% proof stress of each angle of as-received and 450°C annealed specimens. In both annealing conditions, 0.2% proof stress has anisotropy. Though ultimate tensile stress and maximum strain decreases their anisotropy of all angles by annealing, 0.2% proof stress changes of only 60° to 90° by annealing. In these angle, 0.2% proof stress become high by annealing, and it can be said that anisotropy become even strong in this part. In 0° to 45°, the value of 0.2% proof stress is almost the same in each annealing condition. It is the highest in 0° of all angles and gradually decreases to 45°.

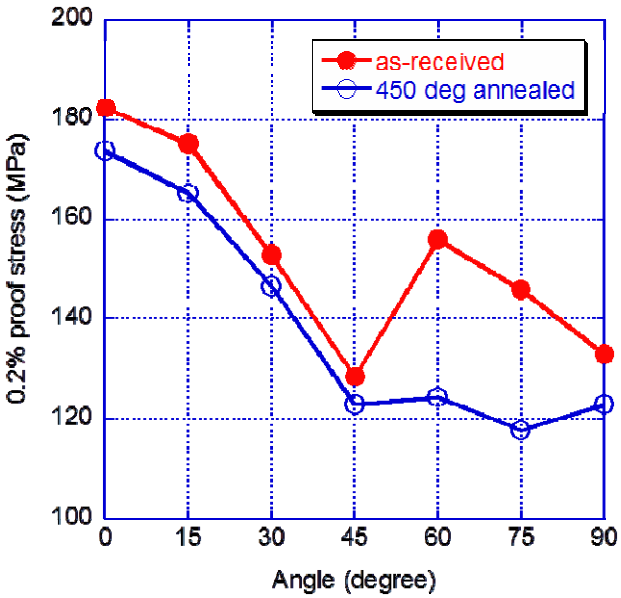

Figure 7. 0.2% proof stress of each angle of as-received and 450°C annealed specimens

3.3. AE measurement

AE result is show in Fig. 8 and Fig. 9. AE measurement was conducted during the tensile test, from start of the test to just before fracture. In each graph, AE result and time stress curve are plotted together in order to connect result of AE measurement and mechanical properties. *x* axis is time, *y* axis is nominal stress and peak frequency of AE signals, and *z* axis is magnitude of AE signals. The value of peak frequency and magnitude is used after wavelet transformed. In all specimens, AE magnitude is high at yield point, so main AE source is related to yielding mechanism. After that, AE magnitude becomes lower gradually as strain increase. In both Fig. 8 and Fig. 9, there are many resemble point. AE magnitude is far higher in 90° than 0° and 45°. Peak frequency is wide range in yield point, but after yielding, AE magnitude is high in high frequency, from about 500 kHz to 600 kHz. The second highest AE magnitude is in frequency of about 300 kHz. In 0°, maximum strain is lowest of all angles, so AE signals is detected in the early time. After annealing, these tendencies are the same. However, AE magnitude of 0° becomes much lower than 45° and 90°.

In order to analyze this AE result, the relationship between AE energy and nominal stress is plotted in Fig. 10. AE energy is calculated as square of AE magnitude and this AE signal is released when nominal stress increases 1 MPa. In Fig 10(a) to (c), AE energy peak (E_{peak}) is extremely high in 90°. AE energy is released from low nominal stress, about 50 MPa, to high nominal stress, about 250 MPa. It is well explained by the fact that AE signals are released at yield point of each specimen.

The nominal stress where AE energy is peak (σ_{AEp}) is low in 90° compared with 0° and 45°. The nominal stress at which AE energy starts to be released ($\sigma_{AEstart}$) is also low, in 90°.

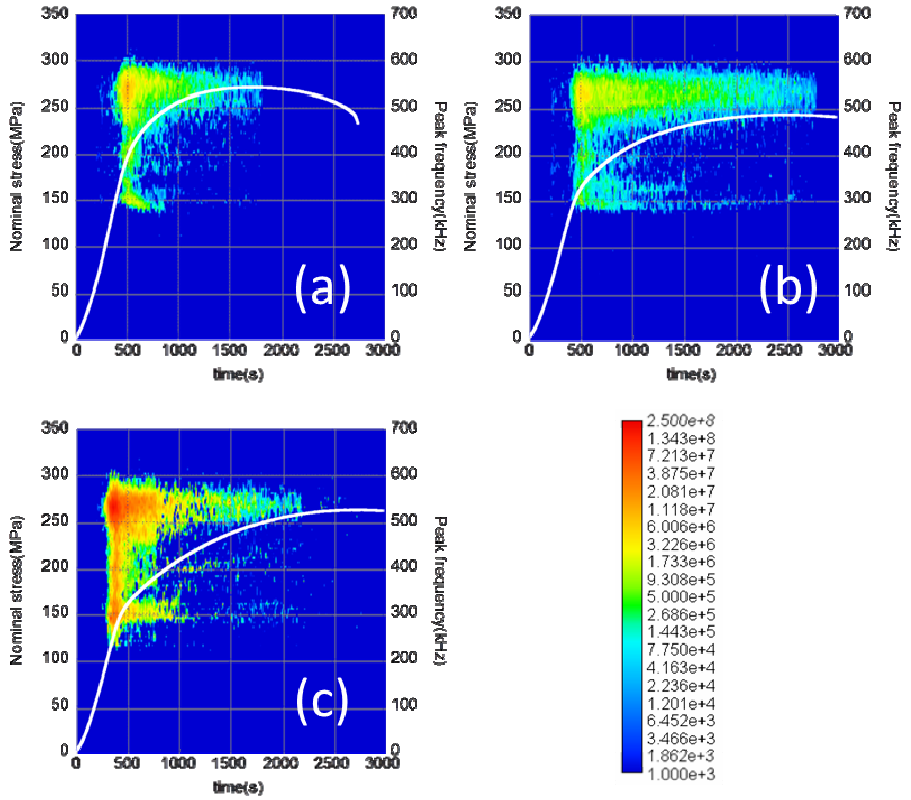

Figure 8. AE magnitude and peak frequency of as-received specimen of (a) 0°, (b) 45° and (c) 90°

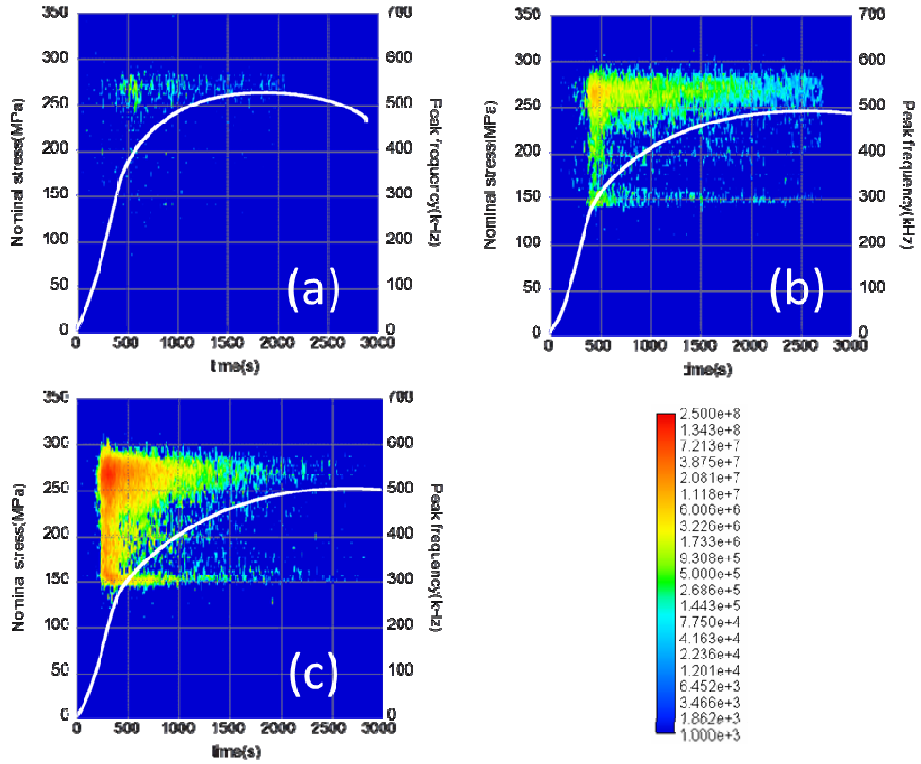

Figure 9. AE magnitude and peak frequency of 450°C annealed specimen of (a) 0°, (b) 45° and (c) 90°

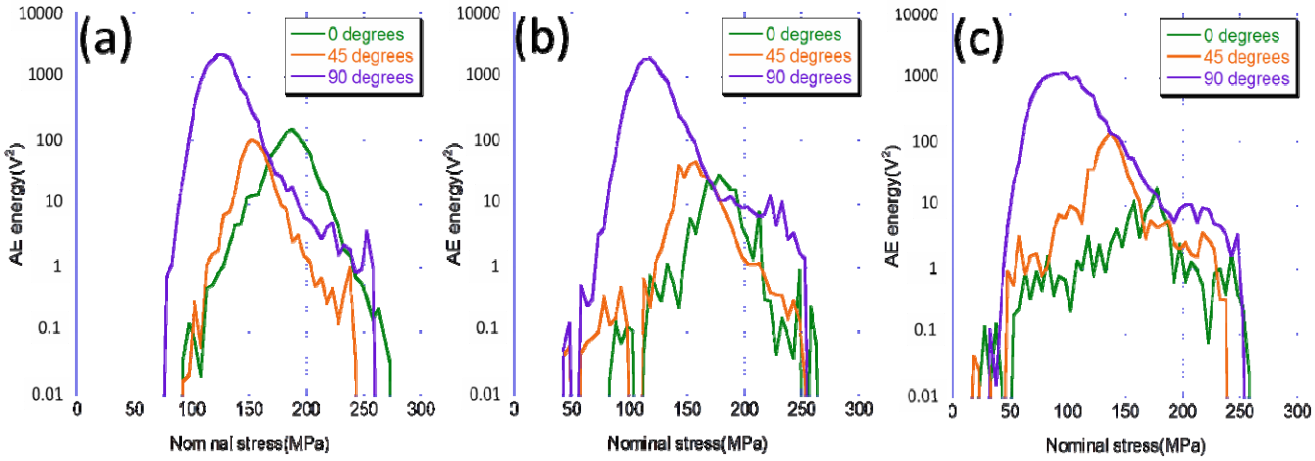

Figure 10. AE energy peak of (a) as-received, (b) 285°C annealed and (c) 450°C annealed specimen

For detail analysis, σ_{AEp} and E_{peak} is plotted in Fig. 11. In each annealing condition, σ_{AEp} become lower and E_{peak} become higher as the angle increases. This tendency is the same in each annealing condition, as-received, 285°C annealed and 450°C annealed. The value is also almost the same. It can be said that σ_{AEp} become lower and E_{peak} become higher when the angle is large for some reason of deformation mechanism.

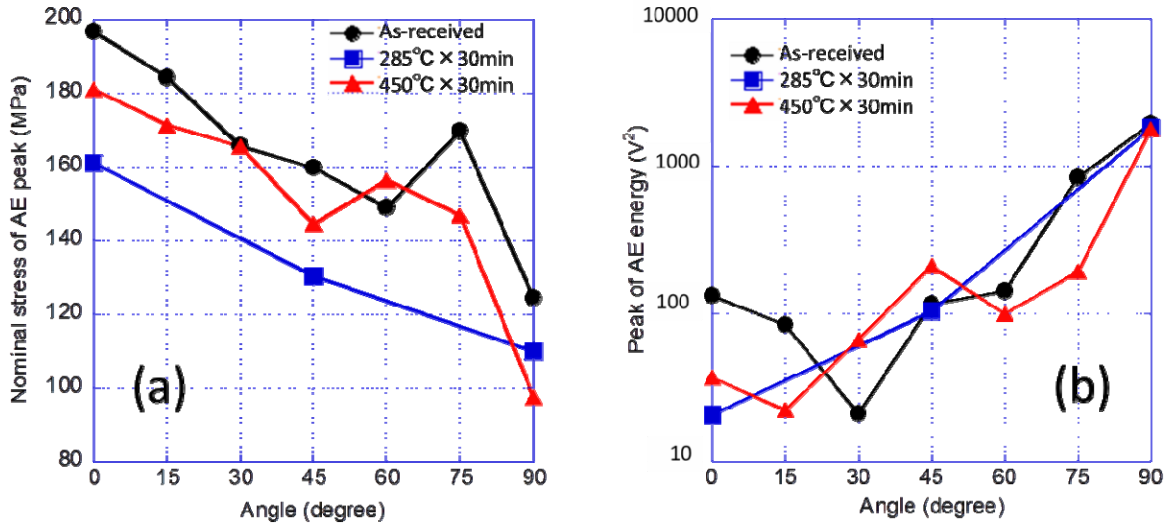

Figure 11. Relationship between tensile angle and (a) nominal stress of AE peak and (b) peak of AE energy of each specimen

In order to see why σ_{AEp} become lower and E_{peak} become higher when the angle is large, x axis is changed to Schmid factor for twinning in Fig. 12. By changing x axis from angle to Schmid factor for twinning, the AE result is connected with mechanical behavior. The abstract of graph is the same as Fig. 10, so it can be said that when Schmid factor for twinning is large, nominal stress of AE peak is low and peak of AE energy is high. The AE result is mainly caused by twinning deformation. When Schmid factor for twinning is large, twinning deformation occurs easily. At low nominal stress twinning deformation occurs, so AE signals released by twinning are detected at lower stress. For the same reason, peak of AE energy is high because the ease of twinning deformation occurring makes more twinning deformation.

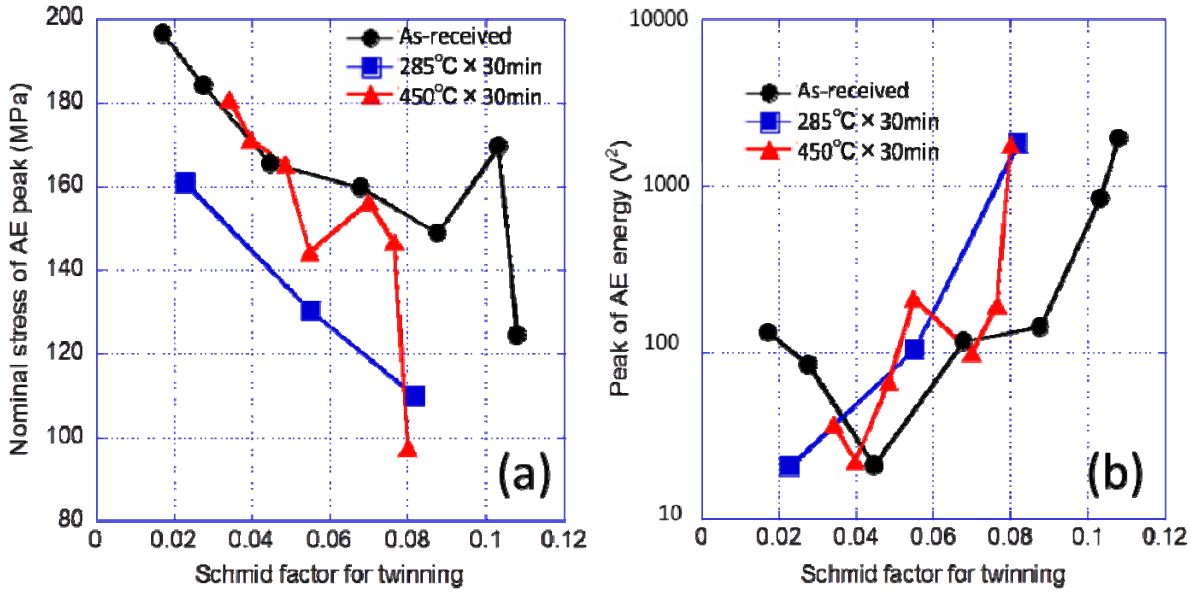

Figure 12. Relationship between Schmid factor for twinning and (a) nominal stress of AE peak and (b) peak of AE energy of each specimen

Fig. 13 shows $\sigma_{AEstart}$ of each angle and each annealing condition. $\sigma_{AEstart}$ is defined as the stress at which AE energy is over 0.01 V^2. At this point, AE energy is especially higher than noise level, and it is easily said that AE energy is released by certain mechanical behavior other than noise. After annealing, in both 285°C and 450°C, $\sigma_{AEstart}$ is almost the same, and the value is less than 20 MPa. However, before annealing, $\sigma_{AEstart}$ is over 30 MPa and has anisotropy. It can be said that when annealed, nominal stress at which AE energy starts to be released is lower and has weaker anisotropy.

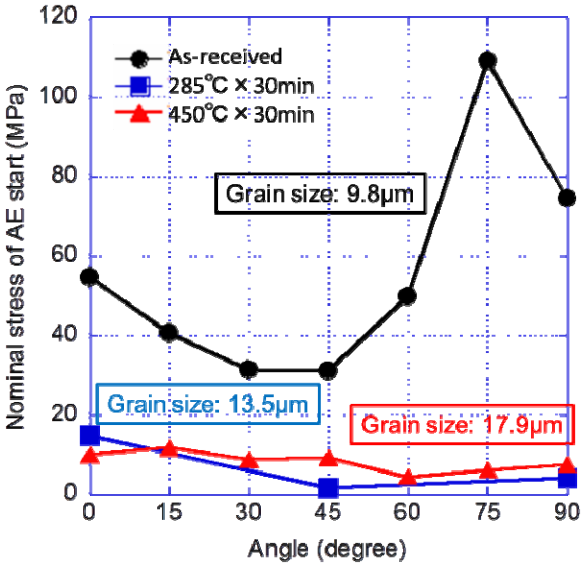

Figure 13. Nominal stress of AE start of each specimen

Fig. 14(a) plotted the relationship between grain size and σ_{AEp}. D is an average grain size, d to the negative one-half power. By annealing, d become larger and D becomes smaller. In each angle, there is linear relationship between D and σ_{AEp}. In other words, Hall-Petch equation, which is shown below, is formed in this result;

.

k, the slope of this equation is larger as the angle increases. Fig. 14(b) shows relationship between *k* and Schmid factor for twinning. In each annealing condition, *k* become larger as Schmid factor for twinning is larger. When Schmid factor for twinning is large, twinning deformation can easily occur, and AE signals are dominated by twinning deformation. Additionally, slope of Hall-Petch equation is larger in twinning than that in slip [8]. For these reason, there is linear relationship between Schmid factor for twinning and k.

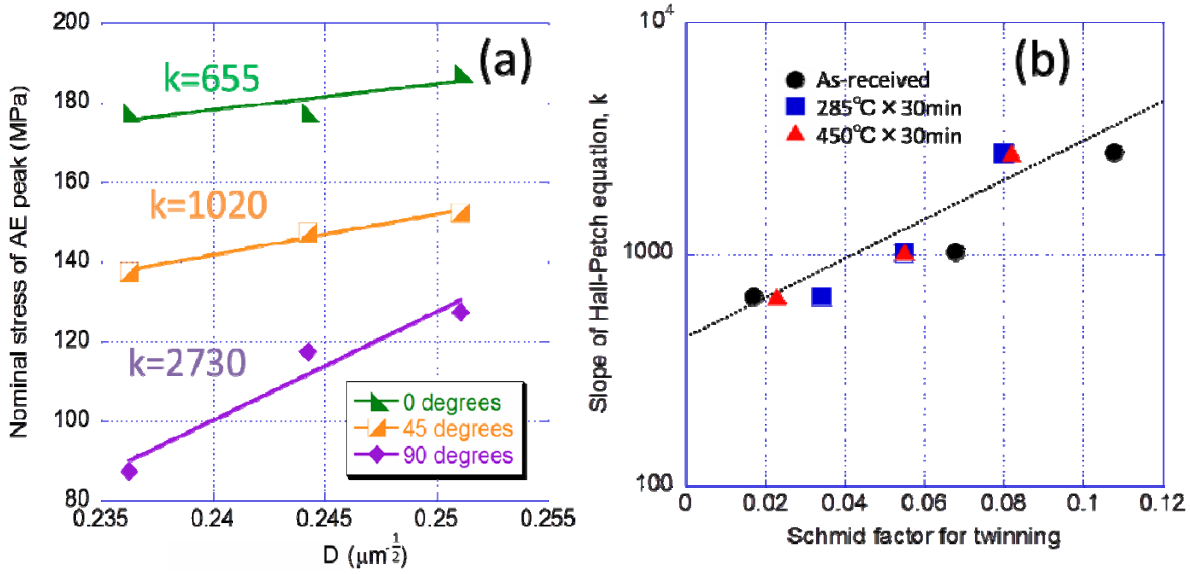

Figure 14. (a) Hall-Petch equation and (b) relationship between slope of the equation and Schmid factor for twinning

4. Conclusion

In the present study, microstructure effect on mechanical properties of AZ31 extruded magnesium alloy is evaluated by AE test and EBSD test, and following conclusions were drawn;

(1) The result of tensile test showed that anisotropy of mechanical properties is weakened by annealing.

(2) Nominal stress of AE energy peak and peak of AE energy were dominated by twinning deformation, so these value changed as Schmid factor for twinning changed.

(3) Nominal stress of AE start showed strong annealing dependence. After annealing, the stress was less than 20 MPa and anisotropy disappeared.

(4) The relationship between nominal stress of AE peak and grain size was well explained by Hall-Petch equation.

(5) Slope of Hall-Petch equation changed as Schmid factor for twinning because twinning deformation is main mechanical behavior in this study.

References

[1] T. Yasutomi and M. Enoki, In-situ evaluation of detwinning behavior in extruded AZ31 mg alloy by AE. Materials Transactions, 53(2012) 1611-1616.

[2] Y. P. Li and M. Enoki, Evaluation of the Twinning Behavior of Polycrystalline Magnesium at Room Temperature by Acoustic Emission. Materials Transactions, 48(2007) 1215-1220.

[3] Y. P. Li and M. Enoki, Deformation and Anelastic Recovery of Pure Magnesium and AZ31B Alloy Investigated by AE. Materials Transactions, 48(2007) 2343-2348.
[4] Y. P. Li and M. Enoki, Recovery Behaviour of Pure Magnesium in Cyclic Compression–Quick Unloading-Recovery Process at Room Temperature Investigated by AE. Materials Transactions, 49(2008) 1800-1805.
[5] Y. P. Li and M. Enoki, Twinning behavior of pure magnesium quantitatively investigated by acoustic emission. Materials Science and Engineering, 536(2012) 8-13.
[6] Y. P. Li and M. Enoki, Anelastic recovery of pure magnesium quantitatively evaluated by acoustic emission. Journal of Materials Research, 26(2011) 3098-3106.
[7] K. Ito and M. Enoki, Acquisition and Analysis of Continuous Acoustic Emission Waveform for Classification of Damage Sources in Ceramic Fiber Mat. Materials Transactions, 48(2007) 1221-1226.
[8] M.R. Barnett, Z. Keshavarz, A.G. Beer and D. Atwell, Influence of grain size on the compressive deformation of wrought Mg-3Al-1Zn. Acta Materialia, 52(2004) 5093-5103.